

GALAXY MODELS WITH TANGENTIALLY ANISOTROPIC VELOCITY DISTRIBUTIONS

J. H. A.¹ N. W. E

Institute of Astronomy, University of Cambridge, Madingley Road, Cambridge CB3 0HA, UK;
jinan@space.mit.edu, nwe@ast.cam.ac.uk
the Astronomical Journal

ABSTRACT

This paper provides two families of flexible and simple galaxy models. Many representatives of these families possess important cosmological cusps, with the density behaving like r^{-1} , $r^{-4/3}$, or $r^{-3/2}$ at small radii. The density falls off between r^{-3} and r^{-5} at large radii. We provide analytic and anisotropic distribution functions for all the models. Unlike many existing methods, our algorithm can yield tangentially anisotropic velocity dispersions in the outer parts, and so is useful for modeling populations of satellite galaxies and substructure in host galaxy halos. As an application, we demonstrate the degeneracy between mass and anisotropy for the satellite galaxy population of the Milky Way. This can introduce a factor of ~ 3 uncertainty in the mass of the Milky Way as inferred from the kinematics of the satellite population.

Subject headings: galaxies: kinematics and dynamics— methods: analytical – stellar dynamics

1. INTRODUCTION

One of Eddington's famous discoveries is that the isotropic distribution function (DF) of a spherical stellar system can be calculated from the density using an Abel transform pair (Eddington 1916; Binney & Tremaine 1987, p. 237):

$$f(E) = \frac{1}{\sqrt{8}\pi^2} \left(\int_0^E \frac{d^2\rho}{d\psi^2} \frac{d\psi}{\sqrt{E-\psi}} + \frac{1}{\sqrt{E}} \frac{d\rho}{d\psi} \Big|_{\psi=0} \right). \quad (1)$$

Here, $E = \psi - v^2/2$ is the binding energy per unit mass, and ψ is the relative potential.

However, galaxy halos produced in cosmological simulations are held up by anisotropic velocity dispersions (see e.g., Hansen & Moore 2006). The recovery of an anisotropic DF for a spherical system is a more difficult problem (Hunter & Qian 1993). Now, the steady state DF can depend not only on E but also on the magnitude of the specific angular momentum $L = rv_T$ through Jeans' theorem. Here v_T is the two-dimensional velocity component projected on the tangential plane.

At least in the comparison of observational data with models (e.g., van der Marel et al. 2000; Wilkinson et al. 2004; Treu & Koopmans 2004), a widely used *Ansatz* for the form of DF is

$$f(E, L) = L^{-2\beta} f_E(E), \quad (2)$$

where $f_E(E)$ is a function of the binding energy alone. It is easy to show that the models generated by this DF exhibit the property that

$$\beta = 1 - \frac{\langle v_T^2 \rangle}{2\langle v_r^2 \rangle}. \quad (3)$$

Here, $\langle v_r^2 \rangle$ and $\langle v_T^2 \rangle$ are the radial and the tangential velocity second moments. The general inversion formula for the unknown function $f_E(E)$ (Cuddeford 1991; Kochanek 1996; Wilkinson & Evans 1999, see also Appendix A) is no more difficult than Eddington's formula (eq. 1).

We note that it is common practice to characterize the velocity anisotropy of a spherically symmetric stellar system by the parameter β defined in equation (3), which is sometimes referred to as the anisotropy parameter (Binney & Tremaine 1987). If $0 < \beta \leq 1$, the velocity dispersion ellipsoid is a prolate spheroid with the major axis along the radial direction (radially anisotropic), while it is an oblate spheroid with the tangential plane being the plane of symmetry (tangentially anisotropic) if $\beta < 0$. In particular, $\beta = 1$ and $\beta = -\infty$ indicate that every star is in a radial or circular orbit, respectively. On the other hand, systems with isotropic velocity dispersions have $\beta = 0$. In general, the anisotropy parameter varies radially, but for the system with a DF of the form of equation (2), it is constant everywhere.

Despite the attractiveness of a simple inversion of the DF in equation (2), the assumption of uniform anisotropy is not always desirable. For example, it is useful to be able to build models that are isotropic in the center and radially anisotropic in the outer parts, as seems to be the case for dark matter halos (Hansen & Moore 2006). DFs that are tangentially anisotropic in the outer parts are helpful for understanding the substructure and the satellite galaxy populations in dark matter halos.

In this paper we study algorithms for building galaxies with varying anisotropy, using sums of DFs of the form of equation (2). § 2 introduces a new family of cusped halo models, the generalized isochrones, and § 3 examines the generalized Plummer models. Every member of the family has analytic potential-density pairs, velocity dispersions, and DFs. Specific examples are provided with the cosmologically important r^{-1} , $r^{-3/2}$, and $r^{-4/3}$ density cusps. § 4 discusses a specific application of our

¹ Current Address: MIT Kavli Institute for Astrophysics & Space Research, Massachusetts Institute of Technology, 77 Massachusetts Avenue, Cambridge, MA 02139, USA

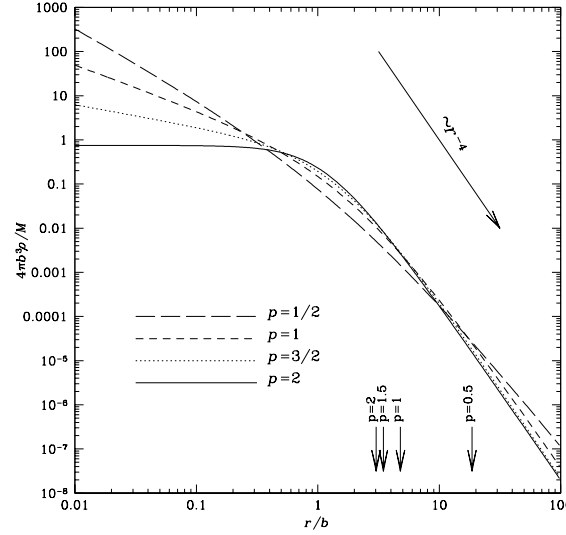


FIG. 1.— Density profile of the generalized isochrone models. The classical isochrone ($p = 2$) is cored, whereas all other models are cusped with $\rho \sim r^{-(p-2)}$ at small radii. The small arrows indicate the half-mass radius.

theoretical models to the problem of estimating the mass of a host galaxy from the motion of its satellites. Finally, § 5 concludes with a brief comparison between our methods of producing varying-anisotropy DFs and other suggestions in the literature (e.g., Osipkov 1979; Merritt 1985; Cuddeford 1991; Gerhard 1991).

2. THE GENERALIZED ISOCHRONE SPHERES

The isochrone sphere has the potential-density pair (Hénon 1959; Eggen, Lynden-Bell, & Sandage 1962; Evans, de Zeeuw, & Lynden-Bell 1990)

$$\psi = \frac{GM}{b+s}; \quad \rho = \frac{M}{4\pi} \frac{(2s+b)b}{s^3(b+s)^2}, \quad (4)$$

where M is the total mass of the system, $s = \sqrt{b^2 + r^2}$, and b is a constant defining the scale length. Like the Plummer (1911) model, the density is finite and well behaved at the center. Unlike the Plummer model, the density falls off as r^{-4} at large radii, which is a better fit to elliptical galaxies than the r^{-5} fall-off of the Plummer model. There are many available studies regarding its DFs (e.g., Gerhard 1991; Bertin et al. 1997), some of which are essentially numerical in nature.

Inspired by this, let us consider the potential-density pair

$$\psi = \frac{GM}{b+s}; \quad \rho = \frac{M}{4\pi} \frac{2br^p + b^p(1+p)(b+s)}{r^{2-p}s^{2p-1}(b+s)^3}, \quad (5)$$

where

$$s = (b^p + r^p)^{1/p}. \quad (6)$$

Here, $p > 0$ is a new parameter used for the generalization of the isochrone sphere (eq. 4). The condition that the density decreases monotonically with increasing radius restricts $p \leq 2$, with the limit ($p = 2$) being the cored classical isochrone sphere. In fact, all the halo models with $0 < p < 2$ are cusped. In particular, the density behaves as $\rho \sim r^{-(2-p)}$ as $r \rightarrow 0$. On the other hand, we find that $\rho \sim r^{-q}$ where $q = \min(4, p+3)$ as $r \rightarrow \infty$. The density profiles of some members of this family are shown in Figure 1. We note that the case $p = 1$, for which $\psi = GM/(2b+r)$, is actually recognized as the Hernquist (1990) model, albeit with a slightly unusual identification for the scale length ($a = 2b$). Models with $p = 1/2$ and $p = 2/3$ possess the cosmological cusps suggested by Moore et al. (1998) and Evans & Collett (1997).

The enclosed mass and the circular speed are found to be

$$M_r = -\frac{r^2}{G} \frac{d\psi}{dr} = M \left(1 + \frac{b^p}{r^p}\right)^{1/p-1} \left[\left(1 + \frac{b^p}{r^p}\right)^{1/p} + \frac{b}{r} \right]^{-2}; \quad v_c^2 = \frac{GM_r}{r} = \frac{GMr^p}{s^{p-1}(b+s)^2}. \quad (7)$$

The potential $\psi(r)$ of the generalized isochrone sphere is simple enough that the inverse, $r(\psi)$, can be easily found (with $G = M = b = 1$ without any loss of generality):

$$r(\psi) = \frac{[(1-\psi)^p - \psi^p]^{1/p}}{\psi}. \quad (8)$$

Using this, in principle, one can construct infinitely many different expressions for $\rho(\psi, r)$, each of which can be inverted to yield the DF by means of integral transforms (Lynden-Bell 1962). However, for most cases this procedure is analytically intractable. Rather, it is often more productive to look for a specific form of $\rho(\psi, r)$ that is associated with a plausible *Ansatz* for the DF, whose inversion reduces to elementary integrals.

2.1. Two Component Distribution Functions

One such possible (r, ψ) -split with an analytically tractable inversion is given by

$$\rho = \frac{p+1}{4\pi} r^{p-2} \psi^{2p+1} (1-\psi)^{1-2p} + \frac{1}{2\pi} r^{2p-2} \psi^{2p+2} (1-\psi)^{1-2p}. \quad (9)$$

We note that a DF of the form of equation (2) can be inverted from an (r, ψ) -split that is a monomial of r , with its power index linearly related to β . By having the (r, ψ) -split given by a linear combination of two monomials of r , the inversion of equation (9) can be achieved by simply extending the known procedure, while the system is no longer restricted to have uniform velocity anisotropy. Inspired by this, let us suppose that the DF is of the form

$$f(E, L) = L^{p-2} f_1(E) + L^{2p-2} f_2(E), \quad (10)$$

where $f_1(E)$ and $f_2(E)$ are functions of E to be determined. Then, the density is found to be

$$\rho = r^{p-2} \frac{2^{p/2+1/2} \pi^{3/2} \Gamma(p/2)}{\Gamma(p/2+1/2)} \int_0^\psi dE (\psi - E)^{p/2-1/2} f_1(E) + r^{2p-2} \frac{2^{p+1/2} \pi^{3/2} \Gamma(p)}{\Gamma(p+1/2)} \int_0^\psi dE (\psi - E)^{p-1/2} f_2(E), \quad (11)$$

where $\Gamma(x)$ is the gamma function. By comparing this to equation (9), a possible DF may be found by inverting the integral equations

$$\begin{aligned} \int_0^\psi dE (\psi - E)^{p/2-1/2} f_1(E) &= \frac{(p+1)\Gamma(p/2+1/2)}{2^{p/2+5/2} \pi^{5/2} \Gamma(p/2)} \psi^{2p+1} (1-\psi)^{1-2p}; \\ \int_0^\psi dE (\psi - E)^{p-1/2} f_2(E) &= \frac{\Gamma(p+1/2)}{2^{p+3/2} \pi^{5/2} \Gamma(p)} \psi^{2p+2} (1-\psi)^{1-2p}. \end{aligned} \quad (12)$$

The inversion procedure is essentially identical to the one that leads to equations (A2) and (A3). After this inversion, we find that $f_1(E)$ and $f_2(E)$ are

$$\begin{aligned} f_1(E) &= \frac{\Gamma(2p+3)}{2^{p/2+7/2} \pi^{5/2} \Gamma(p/2) \Gamma(3p/2+3/2)} E^{(3p+1)/2} {}_2F_1\left(2p-1, 2p+2; \frac{3p+3}{2}; E\right); \\ f_2(E) &= \frac{\Gamma(2p+3)}{2^{p+3/2} \pi^{5/2} \Gamma(p) \Gamma(p+5/2)} E^{p+3/2} {}_2F_1\left(2p-1, 2p+3; p+\frac{5}{2}; E\right), \end{aligned} \quad (13)$$

both of which are always nonnegative for all accessible E -values ($0 \leq E \leq \psi \leq 1/2$). While we have given the result in complete generality in terms of hypergeometric functions ${}_2F_1(a, b; c; x)$, the DFs reduce to entirely elementary and analytic functions if $p = 1/2, 1$, or 2 . In fact, if $p = 1/2$, both hypergeometric functions are just unity, whereas if p is an integer, both reduce to elementary functions. If p is a half integer other than $1/2$, only f_2 reduces to an elementary function.

Of particular interest is the case in which $p = 1/2$, for which the model possesses a central cusp like $\rho \sim r^{-3/2}$, as found by cosmological simulations (Moore et al. 1998). The corresponding DF is very simple, namely,

$$f(E, L) = \frac{3}{4\pi^3} \frac{E^2}{L} + \frac{2^{5/4} \cdot 3}{5\pi^{5/2} \Gamma(1/4)^2} \frac{E^{5/4}}{L^{3/2}}. \quad (14)$$

If $p = 1$ (the Hernquist model with a rescaled scale length),

$$f(E, L) = \frac{1}{2^{7/2} \pi^3 (1-E)^2} \left[\frac{3 \arcsin \sqrt{E}}{\sqrt{1-E}} - (1-2E)(3+8E-8E^2) \sqrt{E} \right] + \frac{1}{4\pi^3 L} \frac{E^2(3-2E)}{(1-E)^2}, \quad (15)$$

or if $p = 2$ (the classical isochrone sphere);

$$\begin{aligned} f(E, L) &= \frac{3L^2}{2^{17/2} \pi^3 (1-E)^5} \left[(40E^2 - 24E + 5) \frac{15 \arcsin \sqrt{E}}{\sqrt{1-E}} - (75 - 310E + 400E^2 - 928E^3 + 576E^4 - 128E^5) \sqrt{E} \right] \\ &+ \frac{3}{2^{15/2} \pi^3 (1-E)^4} \left[(16E^2 - 12E + 3) \frac{15 \arcsin \sqrt{E}}{\sqrt{1-E}} - (45 - 150E + 144E^2 - 208E^3 + 64E^4) \sqrt{E} \right]. \end{aligned} \quad (16)$$

Both of these DFs are no more complicated than the isotropic DFs deduced by Hernquist (1990) and Hénon (1960), respectively.

2.1.1. Kinematics

To find the velocity dispersion of these models, we exploit the splitting $\rho = \rho_1 + \rho_2$, where

$$\rho_1 = \int L^{p-2} f_1(E) d^3\mathbf{v} = \frac{(p+1)r^{p-2}\psi^{2p+1}(1-\psi)^{1-2p}}{4\pi}; \quad \rho_2 = \int L^{2p-2} f_2(E) d^3\mathbf{v} = \frac{r^{2p-2}\psi^{2p+2}(1-\psi)^{1-2p}}{2\pi}. \quad (17)$$

Then,

$$\rho \langle v_r^2 \rangle = \frac{\rho_1 \psi}{2(p+1)} V_1 + \frac{\rho_2 \psi}{2p+3} V_2; \quad \rho \langle v_T^2 \rangle = \frac{p\rho_1 \psi}{2(p+1)} V_1 + \frac{2p\rho_2 \psi}{2p+3} V_2, \quad (18)$$

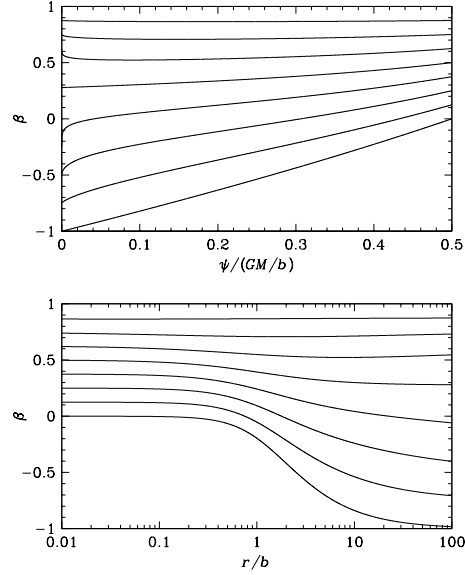


FIG. 2.— Behavior of the anisotropy parameter generated by the DFs (eq. 10) for the generalized isochrone spheres. From top to bottom, the parameter p varies from $1/4$ to 2 with increments of $1/4$. Note that the last curve, $p = 2$, corresponds to the classical cored isochrone sphere.

where

$$V_i = (1 - \psi) {}_2F_1(3 + i, 1; 2p + 2 + i; \psi) = {}_2F_1\left(2p - 1, 1; 2p + 2 + i; -\frac{\psi}{1 - \psi}\right). \quad (19)$$

The anisotropy parameter

$$\beta = 1 - \frac{p}{2} \left[\frac{(2p + 3)V_1 + 8r^p \psi V_2}{(2p + 3)V_1 + 4r^p \psi V_2} \right] \quad (20)$$

is now no longer constant. Figure 2 shows the behavior of β for some of these models. The curves can be understood on examination of equation (20). This reveals that whereas $\beta = 1 - (p/2)$ at $r = 0$ for any p , $\lim_{r \rightarrow \infty} \beta = 1 - p$ if $p > 1$, or $\lim_{r \rightarrow \infty} \beta = 1 - (p/2)$ if $p < 1$. At the critical value $p = 1$, we find that the anisotropy parameter monotonically decreases from $\beta = 1/2$ at $r = 0$ to $\beta \rightarrow 5/18$ as $r \rightarrow \infty$. Hence, the DFs discussed in this section build the generalized isochrone spheres with either decreasing β in the inner region and increasing β in the outer region ($p < 1$), or decreasing β throughout ($p \geq 1$). The particular case of the latter also includes the Hernquist model ($p = 1$) and the classical isochrone sphere ($p = 2$).

The simplest case is again $p = 1/2$, which leads to

$$\langle v_r^2 \rangle = \frac{4\rho_1 + 3\rho_2}{\rho_1 + \rho_2} \frac{\psi}{12} = \frac{2 + 3r^{1/2} + r}{6 + 10r^{1/2} + 3r} \psi; \quad \langle v_T^2 \rangle = \frac{2\rho_1 + 3\rho_2}{\rho_1 + \rho_2} \frac{\psi}{12} = \frac{2 + 4r^{1/2} + r}{6 + 10r^{1/2} + 3r} \frac{\psi}{2}. \quad (21)$$

Then we find that the virial theorem holds locally for this case:

$$\langle v_r^2 \rangle + \langle v_T^2 \rangle = \frac{6\rho_1 + 6\rho_2}{\rho_1 + \rho_2} \frac{\psi}{12} = \frac{\psi}{2}, \quad (22)$$

and the anisotropy parameter

$$\beta = \frac{1}{4} \frac{6 + 8r^{1/2} + 3r}{2 + 3r^{1/2} + r} = \frac{3(r - 2)^2 - r^{1/2}(r + 2)}{4(r - 4)(r - 1)} \quad (23)$$

varies from $\beta = 3/4$ at $r = 0$, to $\beta = 1/\sqrt{2}$ at $r = 2$, and back to $\beta \rightarrow 3/4$ as $r \rightarrow \infty$. This model in fact corresponds to one of the generalized hypervirial models studied by An & Evans (2005a). That is, $\psi = [1 + (1 + r^{1/2})^2]^{-1} = (2 + 2r^{1/2} + r)^{-1}$ so that $r_0 = 2b$ and $(p, c) = (1, 1/\sqrt{2})$ in their parameters.

We note that both V_1 and V_2 in fact reduce to the incomplete Beta functions, which may be useful for the purpose of numerical calculations. Furthermore, if $4p$ is an integer, both V_1 and V_2 reduce to elementary functions of ψ , and so do the velocity second moments. In particular, if $p = 1$ [for which $\psi = (2 + r)^{-1}$],

$$\langle v_r^2 \rangle = \frac{1}{2} (1 + r)(2 + r)^3 \ln\left(\frac{2 + r}{1 + r}\right) - \frac{128 + 303r + 250r^2 + 90r^3 + 12r^4}{24(2 + r)}; \quad (24)$$

$$\langle v_T^2 \rangle = \frac{1}{2} (1 + 2r)(2 + r)^3 \ln\left(\frac{2 + r}{1 + r}\right) - \frac{64 + 217r + 211r^2 + 84r^3 + 12r^4}{12(2 + r)}. \quad (25)$$

3. GENERALIZED PLUMMER MODELS

Next, let us consider the one-parameter family of potential-density pairs,

$$\psi = \frac{GM}{(a^p + r^p)^{1/p}}; \quad \rho = \frac{(p+1)M}{4\pi} \frac{a^p}{r^{2-p}(a^p + r^p)^{2+1/p}}, \quad (26)$$

which was originally introduced by Veltmann (1979). This includes the Hernquist (1990) model ($p = 1$) and the Plummer (1911) model ($p = 2$) as particular cases. Evans & An (2005) recently found that this family can be constructed from power-law DFs of the form of $f(E, L) \propto L^{p-2} E^{(3p+1)/2}$. Here we construct slightly more complicated DFs that build this family of models. We first find every DF of the form of equation (2), and then use them to build models with a more general variation of anisotropy.

3.1. Distribution Functions with Constant Anisotropy Parameter

With $G = M = a = 1$, we find that

$$r^{2\beta} \rho = \frac{p+1}{4\pi} \psi^{p+3-2\beta} (1 - \psi^p)^{1-2(1-\beta)/p}, \quad (27)$$

and that

$$\left. \frac{d^m}{d\psi^m} (r^{2\beta} \rho) \right|_{\psi=0} = 0 \quad (28)$$

for $m < p + 3 - 2\beta$. Then, equation (A2) reduces to

$$f(E, L) = \frac{2^{\beta-1}}{(2\pi)^{5/2}} \frac{p+1}{\Gamma(n-\beta-1/2)\Gamma(1-\beta)} \frac{1}{L^{2\beta}} \frac{d^{n+1}}{dE^{n+1}} \int_0^E \frac{\psi^{p+3-2\beta}}{(1-\psi^p)^\lambda} \frac{d\psi}{(E-\psi)^{3/2-\beta-n}}, \quad (29)$$

where $n = \lfloor 3/2 - \beta \rfloor$ is the integer floor of $3/2 - \beta$, and $\lambda + 1 = 2(1 - \beta)/p$. If $\lambda \geq 0$, it is at least formally possible to derive the series expression of the DF for arbitrary p and β from the integral form, namely,

$$f(E, L) = \frac{2^{\beta-1}}{(2\pi)^{5/2}} \frac{p+1}{\Gamma(1-\beta)} \frac{E^{p+3/2-\beta}}{L^{2\beta}} \sum_{k=0}^{\infty} \frac{\Gamma(pk + p + 4 - 2\beta)}{\Gamma(pk + p + 5/2 - \beta)} \frac{\Gamma(k + \lambda)}{\Gamma(\lambda)} \frac{E^{pk}}{k!}, \quad (30)$$

which becomes the generalized hypergeometric series if p is a rational number. On the other hand, if $-1 < \lambda < 0$, we find that $\lim_{E \rightarrow 1^-} f(E, L) < 0$ so that the corresponding DF is unphysical. Hence, for the potential-density pair of equation (26), the constant anisotropy DF is physical only if $p \leq 2(1 - \beta)$. This means that the hypervirial models of Evans & An (2005), which have an anisotropy parameter $\beta = 1 - (p/2)$, have the maximally radially biased velocity dispersions for a given p and a constant β . Although there exist models with β locally exceeding $1 - (p/2)$ for the generalized Plummer sphere of given p (see e.g., Baes & Dejonghe 2002), β at the center cannot be greater than $1 - (p/2)$ for physically valid DFs. This is in agreement with the cusp slope–central anisotropy theorem derived by An & Evans (2005b).

The corresponding velocity dispersions can be found either from equation (A8) or by solving Jeans equation. The results can be generally expressed using the incomplete Beta functions. The equivalent results expressed in terms of hypergeometric functions are also found in equation (9) of Evans & An (2005).

For particular values of p or β , the DF of equation (29) (or equivalently, eq. 30) reduces to a simpler form. For example, if $\beta = 1/2$, the DF is (see eq. A3)

$$f(E, L) = \frac{p+1}{(2\pi)^3 L} \frac{E^{p+1}}{(1 - E^p)^{1/p}} [(p+2) - (2p+1)E^p], \quad (31)$$

where the positive definiteness of the DF implies that $0 < p \leq 1$. Similarly, for $\beta = -1/2$, the DF is

$$f(E, L) = \frac{(p+1)L}{(2\pi)^3} \frac{E^{p+2}}{(1 - E^p)^{1+3/p}} [(p+3)(p+4) - (5p^2 + 12p + 3)E^p + 2p(2p+1)E^{2p}], \quad (32)$$

which is nonnegative for $0 \leq E \leq 1$ if $0 < p \leq 3$. On the other hand, the DF of the Hernquist model with constant β reduces to the hypergeometric function (see e.g., Baes & Dejonghe 2002)

$$f(E, L) = \frac{2^\beta \Gamma(5 - 2\beta)}{(2\pi)^{5/2} \Gamma(7/2 - \beta) \Gamma(1 - \beta)} \frac{E^{5/2-\beta}}{L^{2\beta}} {}_2F_1\left(1 - 2\beta, 5 - 2\beta; \frac{7}{2} - \beta; E\right), \quad (33)$$

which is nonnegative everywhere if $\beta \leq 1/2$, whereas that for the constant- β Plummer model reduces to

$$f(E, L) = \frac{3 \cdot 2^{\beta-1} \Gamma(6 - 2\beta)}{(2\pi)^{5/2} \Gamma(9/2 - \beta) \Gamma(1 - \beta)} \frac{E^{7/2-\beta}}{L^{2\beta}} {}_3F_2\left(-\beta, 3 - \beta, \frac{7}{2} - \beta; \frac{9 - 2\beta}{4}, \frac{11 - 2\beta}{4}; E^2\right), \quad (34)$$

which is physical if $\beta \leq 0$.

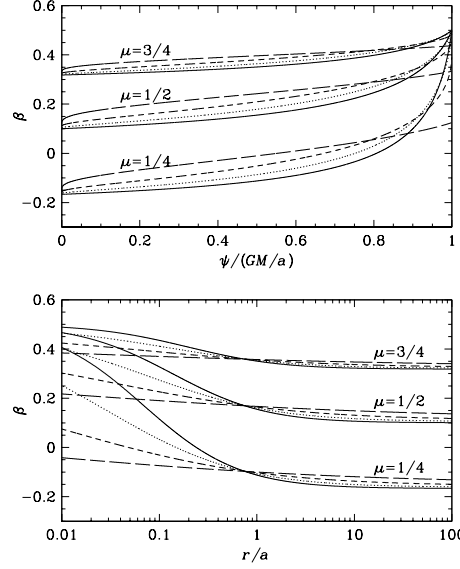


FIG. 3.— Behavior of the anisotropy parameter generated by the DFs (eq. 42) for the generalized Plummer models. Solid lines, $p = 1$ (Hernquist model); dotted lines, $p = 3/4$; short-dashed lines, $p = 1/2$; long-dashed lines, $p = 1/4$.

3.2. Distribution Functions with Outwardly Decreasing Anisotropy Parameter

Since equation (27) is valid for any constant β with common ρ , it is, in general, also possible to express the density profile of the generalized Plummer model by

$$\rho = \frac{p+1}{4\pi} \sum_i \mu_i r^{-2\beta_i} \psi^{p+3-2\beta_i} (1-\psi^p)^{1-2(1-\beta_i)/p}; \quad \sum_i \mu_i = 1, \quad (35)$$

where the parameters $\mu_i > 0$ are normalized weights. Consequently, the superposition of the constant anisotropy DFs, $f(E, L) = \sum_i \mu_i f_i(E, L)$, still builds the generalized Plummer sphere. Here each $f_i(E, L)$ is given by equation (29) (or equivalently, eq. 30) in which β is replaced by β_i . The velocity second moments for these models are found to be

$$\rho \langle v_r^2 \rangle = \rho \psi \sum_i \frac{\mu_i S(r; p, \beta_i)}{p+4-2\beta_i}; \quad \rho \langle v_T^2 \rangle = \rho \psi \sum_i \frac{2\mu_i(1-\beta_i) S(r; p, \beta_i)}{p+4-2\beta_i}, \quad (36)$$

where

$$S(r; p, \beta) = {}_2F_1\left(\frac{2-2\beta}{p} - 1, 1; \frac{4-2\beta}{p} + 2; -\frac{1}{r^p}\right) = (r\psi)^p {}_2F_1\left(\frac{2}{p} + 3, 1; \frac{4-2\beta}{p} + 2; \psi^p\right), \quad (37)$$

and therefore the anisotropy parameter β is no longer constant.

For the particular case in which the sum only contains two terms (such that $\mu_1 = \mu$, $\mu_2 = 1-\mu$, and $\mu_i = 0$ for all other i values), the anisotropy parameter is

$$\beta = \frac{\beta_1 \mu (p+4-2\beta_2) S(r; p, \beta_1) + \beta_2 (1-\mu) (p+4-2\beta_1) S(r; p, \beta_2)}{\mu (p+4-2\beta_2) S(r; p, \beta_1) + (1-\mu) (p+4-2\beta_1) S(r; p, \beta_2)}, \quad (38)$$

which is a decreasing function of r , provided that $0 < \mu < 1$ and $\beta_1 \neq \beta_2$. If we assume $\beta_2 < \beta_1 \leq 1 - (p/2)$ and $0 < \mu < 1$, the limiting values are found to be

$$\lim_{r \rightarrow \infty} \beta = \frac{\beta_1 \mu (p+4-2\beta_2) + \beta_2 (1-\mu) (p+4-2\beta_1)}{\mu (p+4-2\beta_2) + (1-\mu) (p+4-2\beta_1)}. \quad (39)$$

On the other hand,

$$\beta(r=0) = \beta_1 \quad \text{if } \beta_1 \geq 1-p, \quad (40)$$

or

$$\beta(r=0) = \frac{\beta_1 \mu (1-p-\beta_2) + \beta_2 (1-\mu) (1-p-\beta_1)}{\mu (1-p-\beta_2) + (1-\mu) (1-p-\beta_1)} \quad \text{if } \beta_1 \leq 1-p. \quad (41)$$

The simplest example of the DFs of this kind is obtained when we choose $\beta_1 = 1/2$ and $\beta_2 = -1/2$:

$$f(E, L) = \frac{p+1}{(2\pi)^3} \left[\mu \frac{E^{p+1}}{L} \frac{(p+2) - (2p+1)E^p}{(1-E^p)^{1/p}} + (1-\mu) L E^{p+2} \frac{(p+3)(p+4) - (5p^2 + 12p + 3)E^p + 2p(2p+1)E^{2p}}{(1-E^p)^{1+3/p}} \right], \quad (42)$$

which is physical if $p \leq 1$. The behavior of the anisotropy parameter β for the model given by DFs of equation (42) is shown in Figure 3. Again we note that equation (37) in general reduces to the incomplete Beta function while, for this case, it further reduces to an expression involving only elementary functions of ψ if $2p$ is an integer, and so and so do β and the velocity second moments.

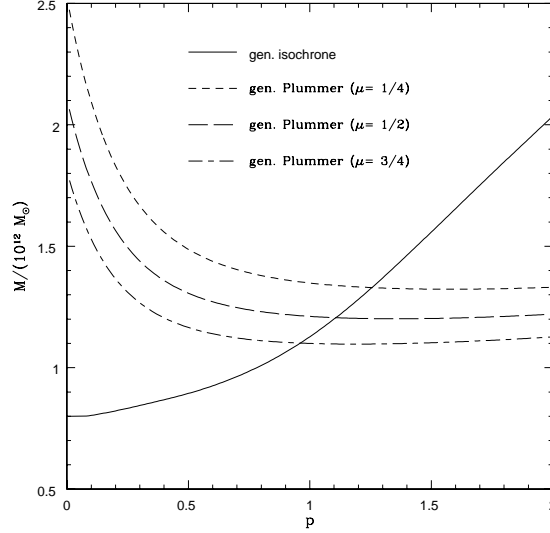


FIG. 4.— Curves illustrating the degeneracy between mass and anisotropy. All the models have the same half-mass radius and reproduce the same mean kinetic energy $\langle T_{rr} \rangle$ of the satellite population of the Milky Way. The inferred mass of the Milky Way (in units of $10^{12} M_{\odot}$) is plotted against the parameter p , which controls the velocity anisotropy.

4. AN APPLICATION: THE MASS OF THE MILKY WAY

As an application of the preceding theory, let us consider the problem of estimating the mass of the Milky Way from the radial velocities of its satellites. There are 27 distant globular clusters and dwarf galaxies at Galactocentric distance r greater than 20 kpc (see e.g., tables 2 and 3 of Wilkinson & Evans 1999). These range from Arp 2 at $r = 20$ kpc out to Leo I at $r = 254$ kpc. The median distance of the satellite population is $r_{\text{med}} \approx 38$ kpc. The number density of the satellites falls off roughly like $r^{-3.5}$. This dataset is often used to estimate the mass of the Milky Way (Kochanek 1996; Wilkinson & Evans 1999), as the H I rotation curve cannot be traced beyond ~ 20 kpc. The satellites are therefore the only available probe of the gravitational field of the distant halo.

All the satellites have accurate radial velocities, but proper motions are available only for a handful of the closest objects. Of course, the heliocentric radial velocity and the Galactocentric radial velocity are basically the same (once the motion of the Sun has been taken out), as the Galactocentric distance of the Sun is much smaller than those of the satellites. The kinematic data therefore constrains the mean kinetic energy in the radial direction $T_{rr} = \langle v_r^2 \rangle$. Again using the data in tables 2 and 3 of Wilkinson & Evans (1999), we find that $T_{rr} \approx (129 \text{ km s}^{-1})^2$.

To model the Milky Way halo, we assume that its potential and density take the form of either the generalized isochrone or the generalized Plummer models. Furthermore, we assume that the number density of satellites shadows the total density (e.g., Kochanek 1996; Wilkinson & Evans 1999). This means that the satellites are drawn from DFs of the form given by either equation (10) or equation (42). We set the scale length so that the half-mass radius of the assumed density profile corresponds to the observed median radius of the population. The mass of the Milky Way M enters into the potential and the DF. It can therefore be constrained by requiring that the mean kinetic energy in the radial direction be consistent with the data, viz,

$$T_{rr} = \frac{\int \rho \langle v_r^2 \rangle d^3\mathbf{r}}{\int \rho d^3\mathbf{r}} \approx 16,640 \text{ km}^2 \text{ s}^{-2}. \quad (43)$$

The parameter p in the DFs controls the variation of the velocity anisotropy with radius. Hence, equation (43) defines a line in the plane (M, p) , which is the *mass-anisotropy degeneracy curve* for the model. Figure 4, inferred from numerical integrations, shows such curves computed for a number of the generalized isochrones and the generalized Plummer models.

In this problem, the mean kinetic energy in the radial direction is fixed. Models with tangential anisotropy at large radii therefore lead to a higher inferred mass for the Milky Way galaxy. The relative location of the curves in Figure 4 can be understood by examining the behavior of the anisotropy parameter for the models. More importantly, as the velocity anisotropy changes, the inferred mass of the Milky Way ranges from $0.8 \times 10^{12} M_{\odot}$ to $2.5 \times 10^{12} M_{\odot}$. Now, the velocity anisotropy of the satellite galaxy population is unknown, so the mass-anisotropy degeneracy *by itself* enforces a factor of ~ 3 uncertainty in the mass of the Milky Way. This fundamental limitation can only be overcome by proper-motion data.

Of course, there are other uncertainties; for example, the half-mass radius of the satellite population used to set the scale length in these calculations is also not well known (note that the locations of the satellites are likely to be biased toward their apogalacticon) and has an uncertainty of $\sim 20\%$. This carries over into an additional $\sim 20\%$ uncertainty in the inferred mass. This is small in comparison with the mass-anisotropy degeneracy, but not insignificantly so.

5. CONCLUSIONS

This paper provides a number of flexible and simple galaxy models extended from two classical cored profiles: the isochrone sphere and Plummer model. We also derive analytic distribution functions (DFs) with varying velocity anisotropy for all the

models including new DFs for the classical isochrone sphere and the Hernquist model.

DFs of the form $f(E, L) = L^{-2\beta} f_E(E)$ build a spherical system with a constant anisotropy parameter β , where E is the binding energy and L is the specific angular momentum. The assumption of constant anisotropy is not enough to provide realistic models, as both observational data and numerical simulations suggest that dark halos and their constituents (such as satellites) have velocity anisotropies that vary with radius (e.g., White 1985; van der Marel 1994; Hansen & Moore 2006).

Here we have explored models whose DFs are superpositions of two or more such terms, namely,

$$f(E, L) = \sum_i L^{-2\beta_i} f_i(E). \quad (44)$$

This can be done in two ways. First, as illustrated by the generalized isochrones in § 2, we can sometimes find a splitting of the density in the form

$$\rho(r) = \sum_i r^{-2\beta_i} g_i(\psi(r)). \quad (45)$$

and apply the inversion separately to each component. For the generalized isochrones, this provides models with either decreasing anisotropy parameter β in the inner region and increasing β in the outer parts, or decreasing β throughout. Second, as illustrated by the generalized Plummer models in § 3, we can always add together weighted sums of constant anisotropy DFs, each of which individually reproduces the required density. This appears to provide models with decreasing anisotropy parameter β throughout. At large radii, the DF is dominated by the component of smallest β , and the models can be either radially or tangentially anisotropic in the outer parts, according to choice. For both cases, it appears that the anisotropy parameter always decreases on beginning to move outward from the very center.

There have been a number of previous algorithms suggested for building anisotropic DFs with varying anisotropy. For example, the Osipkov-Merritt algorithm (Osipkov 1979; Merritt 1985) builds models that are isotropic in the inner parts and tend to extreme radial anisotropy ($\beta \rightarrow 1$) in the outer parts. Gerhard (1991) provided a clever algorithm for building separable DFs of the form

$$f = g(E)h(L/L_c(E)), \quad (46)$$

where L_c is the angular momentum of a circular orbit with energy E . The analytic examples provided by Gerhard (1991) all have increasing radial anisotropy in the outer parts. His method can be used to generate tangentially anisotropic models, but usually at the cost of a numerical inversion. The methods developed in this paper therefore provide a complement to the existing inversions.

Tangential anisotropy often arises in accreted populations, such as satellite galaxies. As an application of our models, we have shown that the mass-anisotropy degeneracy by itself provides a factor ~ 3 uncertainty in the mass of the Milky Way galaxy as deduced from the kinematics of its satellites.

The density profiles of models studied in this paper typically fall off faster than $\rho \sim r^{-3}$ and slower than $\rho \sim r^{-5}$ at large radii, which are in good agreement with both observations of spheroidal components of galaxies and results from numerical simulations. At small radii, they are typically cusped, with cusp indices in the range suggested by numerical simulations. In particular, there are members with density cusps like $\rho \sim r^{-1}$, $\sim r^{-4/3}$, and $\sim r^{-3/2}$, which have been suggested as important on cosmogonic grounds (Navarro, Frenk, & White 1995; Evans & Collett 1997; Moore et al. 1998), although observational evidence seems to favor the presence of a constant-density core (Tyson, Kochanski, & dell'Antonio 1998; Palunas & Williams 2000; de Blok et al. 2001; Kleyna et al. 2003; Donato, Gentile, & Salucci 2004). However, even if real galaxies are cored, the core would be such a small fraction of the halo that it is not practically important for studies of the whole. Our families of new models therefore should find widespread application in the modeling of galaxies and dark halos.

We thank C. Hunter, who made a number of interesting comments on the various incarnations of this paper.

REFERENCES

- An, J., & Evans, N. W. 2005a, *A&A*, 444, 45 (astro-ph/0508419)
 An, J. H., & Evans, N. W. 2005b, *ApJ*, submitted (astro-ph/0511686)
 Baes, M., & Dejonghe, H. 2002, *A&A*, 393, 485
 Bertin, G., Leeuw, F., Pegoraro, F., & Rubini, F. 1997, *A&A*, 321, 703
 Binney, J., & Tremaine, S. 1987, *Galactic Dynamics* (Princeton NJ: Princeton Univ. Press)
 Cuddeford, P. 1991, *MNRAS*, 253, 414
 de Blok, W. J. G., McGaugh, S. S., Bosma, A., & Rubin, V. C. 2001, *ApJ*, 552, L23
 Dejonghe, H. 1987, *MNRAS*, 224, 13
 Donato, F., Gentile, G., & Salucci, P. 2004, *MNRAS*, 353, L17
 Eddington, A. S. 1916, *MNRAS*, 76, 572
 Eggen, O. J., Lynden-Bell, D., & Sandage, A. R. 1962, *ApJ*, 136, 748
 Evans, N. W., & An, J. H. 2005, *MNRAS*, 360, 492 (astro-ph/0501091)
 Evans, N. W., & An, J. H. 2006, *Phys. Rev. D*, submitted (astro-ph/0511687)
 Evans, N. W., & Collett, J. L. 1997, *ApJ*, 480, L103
 Evans, N. W., de Zeeuw, P. T., & Lynden-Bell, D. 1990, *MNRAS*, 244, 111
 Gerhard, O. E. 1991, *MNRAS*, 250, 812
 Hansen, S. H., & Moore, B. 2006, *New A*, 11, 333 (astro-ph/0411473)
 Hénon, M. 1959, *Ann. d'Astrophys.*, 22, 126
 Hénon, M. 1960, *Ann. d'Astrophys.*, 23, 668
 Hernquist, L. 1990, *ApJ*, 356, 359
 Hunter, C., & Qian, E. 1993, *MNRAS*, 262, 401
 Kleyna, J. T., Wilkinson, M. I., Gilmore, G., & Evans, N. W. 2003, *ApJ*, 588, L21
 Kochanek, C. S. 1996, *ApJ*, 457, 228
 Lynden-Bell, D. 1962, *MNRAS*, 123, 447
 Merritt, D. 1985, *AJ*, 90, 1027
 Moore, B., Governato, F., Quinn, T., Stadel, J., & Lake, G. 1998, *ApJ*, 499, L5
 Navarro, J. F., Frenk, C. S., & White, S. D. M. 1995, *MNRAS*, 275, 720
 Osipkov, L. P. 1979, *Pis'ma Astron. Zh.*, 5, 77 (English trans. in *Soviet Astron. Lett.*, 5, 42)
 Palunas, P., & Williams, T. B. 2000, *AJ*, 120, 2884
 Plummer, H. C. 1911, *MNRAS*, 71, 460
 Treu, T., & Koopmans, L. 2004, *ApJ*, 611, 738
 Tyson, J. A., Kochanski, G. P., & dell'Antonio, I. P. 1998, *ApJ*, 498, 107
 van der Marel, R. P. 1994, *MNRAS*, 270, 271
 van der Marel, R. P., Magorrian, J., Carlberg, R. G., Yee, H. K. C., & Ellingson, E. 2000, *AJ*, 119, 2038
 Veltmann, Ü.-I. K. 1979, *AZh*, 56, 976 (English trans. in *Soviet Ast.*, 23, 551)
 White, S. D. M. 1985, *ApJ*, 294, L99
 Wilkinson, M. I., & Evans, N. W. 1999, *MNRAS*, 310, 645
 Wilkinson, M. I., Kleyna, J. T., Evans, N. W., Gilmore, G., Irwin, M. J., & Grebel, E. K. 2004, *ApJ*, 611, 738

APPENDIX

A. CONSTANT ANISOTROPY DISTRIBUTION FUNCTIONS

In this appendix we summarize some results regarding constant-anisotropy DFs used in the main body of the paper. For the DF given in equation (2), direct integration over velocity space gives

$$\rho = r^{-2\beta} \frac{(2\pi)^{3/2} \Gamma(1-\beta)}{2^\beta \Gamma(3/2-\beta)} \int_0^\psi (\psi - E)^{1/2-\beta} f_E(E) dE. \quad (\text{A1})$$

The formula for inversion for the unknown function $f_E(E)$ is given by (Cuddeford 1991)

$$\begin{aligned} f(E, L) &= \frac{1}{L^{2\beta}} \frac{2^\beta}{(2\pi)^{3/2} \Gamma(1-\alpha) \Gamma(1-\beta)} \frac{d}{dE} \int_0^E \frac{d\psi}{(E-\psi)^\alpha} \frac{d^n h}{d\psi^n} \\ &= \frac{1}{L^{2\beta}} \frac{2^\beta}{(2\pi)^{3/2} \Gamma(1-\alpha) \Gamma(1-\beta)} \left[\int_0^E \frac{d\psi}{(E-\psi)^\alpha} \frac{d^{n+1} h}{d\psi^{n+1}} + \frac{1}{E^\alpha} \frac{d^n h}{d\psi^n} \Big|_{\psi=0} \right], \end{aligned} \quad (\text{A2})$$

where $h(\psi) = r^{2\beta} \rho$ is expressed as a function of ψ , and $n = \lfloor 3/2 - \beta \rfloor$ and $\alpha = (3/2 - \beta) - n$ are the integer floor and the fractional part of $3/2 - \beta$, respectively. This includes equation (1) as a particular case of $\beta = 0$ ($n = 1$ & $\alpha = 1/2$). If β is a half-integer constant (i.e., $\beta = 1/2, -1/2, -3/2$, and so on), the above inversion simplifies to

$$f(E, L) = \frac{1}{2\pi^2 L^{2\beta}} \frac{1}{(-2\beta)!!} \left. \frac{d^{3/2-\beta} h}{d\psi^{3/2-\beta}} \right|_{\psi=E}, \quad (\text{A3})$$

that is, this only involves differentiations in the process (Cuddeford 1991). In addition, the expression for the differential energy distribution (DED) is found to be

$$\left. \frac{d\rho}{dE} \right|_{E=E_0} = \int \frac{f_E(E)}{L^{2\beta}} \delta(E - E_0) d^3\mathbf{v} = \frac{(2\pi)^{3/2} \Gamma(1-\beta)}{2^\beta \Gamma(3/2-\beta)} \frac{(\psi - E_0)^{1/2-\beta}}{r^{2\beta}} f_E(E_0) \Theta(\psi - E_0); \quad (\text{A4})$$

$$\frac{dM}{dE} = \int \frac{d\rho}{dE} d^3\mathbf{r} = f_E(E) \frac{(2\pi)^{5/2} \Gamma(1-\beta)}{2^{\beta-1} \Gamma(3/2-\beta)} \int_0^{r_E} (\psi - E)^{1/2-\beta} r^{2(1-\beta)} dr, \quad (\text{A5})$$

where $\psi(r_E) = E$, and $\delta(x)$ and $\Theta(x)$ are the Dirac delta ‘function’ and the Heaviside unit step function, respectively. In particular, if $\beta = 1/2$, the last integral does not explicitly involve the potential, and so the DED may be found simply as $dM/dE = 4\pi^3 r_E^2 f_E(E)$.

It is also straightforward to find the integral for the second velocity moments;

$$\rho \langle v_r^2 \rangle = \frac{(2\pi)^{3/2}}{2^\beta r^{2\beta}} \frac{\Gamma(1-\beta)}{\Gamma(5/2-\beta)} \int_0^\psi (\psi - E)^{3/2-\beta} f_E(E) dE; \quad (\text{A6})$$

$$\rho \langle v_T^2 \rangle = \frac{2(2\pi)^{3/2}}{2^\beta r^{2\beta}} \frac{\Gamma(2-\beta)}{\Gamma(5/2-\beta)} \int_0^\psi (\psi - E)^{3/2-\beta} f_E(E) dE = 2(1-\beta) \rho \langle v_r^2 \rangle. \quad (\text{A7})$$

In fact, the velocity dispersion of any constant anisotropy models may be found from $h(\psi)$ without explicitly evaluating the DF (Dejonghe 1987; Baes & Dejonghe 2002). On differentiating equation (A6) with respect to ψ and noting that the right-hand side is the same as equation (A1), that is, $\partial(\rho \langle v_r^2 \rangle)/\partial\psi = \rho$, it follows that

$$\langle v_r^2 \rangle = \frac{1}{\rho} \int_0^\psi d\psi' \rho(r, \psi') = \frac{1}{h(\psi)} \int_0^\psi d\psi' h(\psi') = \frac{1}{r^{2\beta} \rho} \int_\infty^r dr' \frac{d\psi'}{dr'} r'^{2\beta} \rho. \quad (\text{A8})$$

We note that equation (A8) can also be derived from the integral solution of Jeans’ equation with a constant β (see eq. 9 of Evans & An 2005). This also indicates that equation (A8) is actually a general result for a constant β model, regardless of the specific form of the DF that generates the model.

As an example, let us think of the DFs that build the generalized isochrone sphere with a constant anisotropy parameter. First, the DF and the DED for the generalized isochrone sphere with $\beta = 1/2$ can be found from equation (A3);

$$f(E, L) = \frac{1}{(2\pi)^3 L} \frac{E^2 g(E)}{(1-E)^{2p} [(1-E)^p - E^p]^{1/p}}; \quad \frac{dM}{dE} = \frac{[(1-E)^p - E^p]^{1/p}}{2(1-E)^{2p}} g(E) \quad (\text{A9})$$

$$g(E) = E^{2p-1} [6(p+1)E - 6E^2 - (p+1)(2p+1)] + (1-E)^p E^{p-1} [(p+1)(p+2) + 12E^2 - 6(p+2)E] + 6(1-E)^{2p+1}. \quad (\text{A10})$$

Here, because $0 \leq E \leq \psi \leq 1/2$, the nonnegativity of the DF is satisfied only if $0 < p \leq 1$. In addition, the integration involved in the inversion (eq. A2) is also analytically tractable if $\beta = 1 - (p/2)$. That is, for the density profile of the generalized isochrone sphere, we find that

$$r^{2-p} \rho = \frac{1}{2\pi} \psi^{p+2} (1-\psi)^{1-p} + \frac{1}{8\pi} \frac{d}{d\psi} [\psi^{2p+2} (1-\psi)^{2-2p}]. \quad (\text{A11})$$

This leads to the DF of the form of equation (2)

$$f(E, L) = \frac{1}{L^{2-p}} \frac{1}{2^{p/2+3/2} \pi^{5/2} \Gamma(p/2)} \times \left[\frac{\Gamma(2p+3)}{4\Gamma(3p/2+3/2)} E^{(3p+1)/2} {}_2F_1\left(2p-2, 2p+3; \frac{3p+3}{2}; E\right) + \frac{\Gamma(p+3)}{\Gamma(p/2+5/2)} E^{(p+3)/2} {}_2F_1\left(p-1, p+3; \frac{p+5}{2}; E\right) \right], \quad (\text{A12})$$

which build a constant anisotropy model with $\beta = 1 - (p/2)$.

If $p = 1$ (corresponding to the Hernquist model) and $\beta = 1/2$, the DF and the DED further reduce to a particularly simple form;

$$f(E, L) = \frac{3}{2\pi^3} \frac{E^2}{L}; \quad \frac{dM}{dE} = 6(1-2E)^2, \quad (\text{A13})$$

which was originally found by Baes & Dejonghe (2002) for the Hernquist (1990) model. For $p = 2$ and $\beta = 0$, the well-known expression for the DF of the isotropic isochrone sphere (see e.g., Hénon 1960; Binney & Tremaine 1987, p. 239) is recovered;

$$f(E) = \frac{1}{2^{15/2} \pi^3 (1-E)^4} \left[(16E^2 + 28E - 9) \frac{3 \arcsin \sqrt{E}}{\sqrt{1-E}} + (27 - 66E + 320E^2 - 240E^3 + 64E^4) \sqrt{E} \right]. \quad (\text{A14})$$

Finally, let us think of the DED of the generalized Plummer models corresponding to the DF given in equation (29). For this case, equation (A5) reduces to a similar integral as equation (29)

$$\frac{dM}{dE} = \frac{(2\pi)^{5/2} \Gamma(1-\beta) f_E(E)}{2^{\beta-1}} \frac{1}{\Gamma(3/2-\beta)} \int_E^1 \frac{(1-\psi^p)^{(3-2\beta)/p-1}}{\psi^{2(2-\beta)}} (\psi-E)^{1/2-\beta} d\psi. \quad (\text{A15})$$

Like the DF, equation (A15) reduces to a closed form function of E for particular values of p or β . Among them are for $\beta = 1/2$

$$\frac{dM}{dE} = f_E(E) \frac{(2\pi)^3}{2} \frac{(1-E^p)^{2/p}}{E^2} = \frac{p+1}{2} (1-E^p)^{1/p} [(p+2) - (2p+1)E^p] E^{p-1}, \quad (\text{A16})$$

for $\beta = -1/2$,

$$\begin{aligned} \frac{dM}{dE} &= f_E(E) \frac{(2\pi)^3}{4(p+4)} \frac{(1-E^p)^{1+4/p}}{E^3} {}_2F_1\left(1, \frac{1}{p} + 1; \frac{4}{p} + 2; 1-E^p\right) \\ &= \frac{p+1}{p+4} \frac{(1-E^p)^{1/p}}{4} \left[(p+3)(p+4) - (5p^2 + 12p + 3)E^p + 2p(2p+1)E^{2p} \right] E^{p-1} {}_2F_1\left(1, \frac{1}{p} + 1; \frac{4}{p} + 2; 1-E^p\right), \end{aligned} \quad (\text{A17})$$

and for $p = 1$,

$$\begin{aligned} \frac{dM}{dE} &= f_E(E) \frac{(2\pi)^{5/2} \Gamma(3-2\beta) \Gamma(1-\beta)}{2^{\beta-1} \Gamma(9/2-3\beta)} \frac{(1-E)^{7/2-3\beta}}{E^{5/2-\beta}} {}_2F_1\left(\frac{1}{2}-\beta, \frac{3}{2}-\beta; \frac{9}{2}-3\beta; 1-E\right) \\ &= \frac{2\Gamma(5-2\beta)\Gamma(3-2\beta)}{\Gamma(9/2-3\beta)\Gamma(7/2-\beta)} (1-E)^{7/2-3\beta} {}_2F_1\left(1-2\beta, 5-2\beta; \frac{7}{2}-\beta; E\right) {}_2F_1\left(\frac{1}{2}-\beta, \frac{3}{2}-\beta; \frac{9}{2}-3\beta; 1-E\right). \end{aligned} \quad (\text{A18})$$

This suggests that dM/dE diverges as $E \rightarrow 0$ for $p < 1$, that it vanishes for $p > 1$, and that it has a finite limiting value of $8(2-\beta)/(5-2\beta)$ for $p = 1$. We believe that this is because the behavior of dM/dE near $E = 0$ is dominated by the stars at large radii and the r^{-4} fall-off marks a critical point (Evans & An 2006).